

# MONTE CARLO SIMULATION OF DISPERSIVE CARRIER TRANSPORT IN DISORDERED SOLIDS IN THE PRESENCE OF SPACE CHARGE EFFECTS

WŁADYSŁAW TOMASZEWICZ

*Department of Physics of Electronic Phenomena,  
Faculty of Technical Physics and Applied Mathematics,  
Technical University of Gdansk,  
Narutowicza 11/12, 80-952 Gdansk, Poland  
wtomasze@sunrise.pg.gda.pl*

**Abstract:** A Monte Carlo (MC) method of simulation of the multiple-trapping (MT) carrier transport in disordered solids, taking into account the space charge effects, is presented. The main idea is to utilize the ordered binary trees for the storage of sequences of the carrier positions and release times. An exemplary implementation of MC method in the case of isothermal surface-potential decay is described. Also, modifications of the algorithm for other experimental configurations are indicated. The preliminary simulation results are compared with the approximate solutions of MT transport equations.

## 1. Introduction

One of the characteristic features of disordered semiconductors and insulators is the dispersive character of excess carrier transport (see, for example, the review [1]). When a thin sheet of carriers is generated near the sample surface, the transit times of carriers through the sample under the influence of an external electric field may differ by many orders of magnitude. According to the multiple-trapping (MT) model, the carriers move in the allowed band, being temporarily captured by the localized states (traps) in the energy gap. The origin of dispersive transport is then the distribution of trap energies, which causes a broad dispersion of carrier release times. The investigations of dispersive transport make thus possible to determine the spectrum of trap energies in the forbidden band, which is an important characteristic of amorphous solids.

The majority of experimental and theoretical studies on the subject concern so called small signal regime. This means that the charge generated in the sample is so small that the resulting field distortion may be neglected. The carrier transport equations become then linear, which considerably simplifies the problem. In particular, the MT transport may be easily simulated by the Monte Carlo (MC) method (e.g. [2]). In some circumstances, the space-charge effects may, however, play a significant role.

This concerns particularly the surface-potential decay (SPD) method, which will be described in the next section. Both analytical [3-5] and numerical investigations of the space-charge effects in dispersive transport are difficult. In some papers the problem was treated numerically by the finite-differences method. However, the obtained results were restricted to a relatively small time region [6, 7] or the used algorithms were complicated and not entirely reliable [8]. The more promising approach seems to consist in the suitable extension of the MC method. So far, there has appeared one paper [9], in which the SPD was simulated by the MC technique, but the details of utilized algorithm were not described.

The aim of this paper is to present the method of MC simulation of dispersive carrier transport, taking into account the space charge effects, together with the preliminary results. It should have in mind that the described algorithm is by no means unique and may not be optimal. For example, the use of other data structures might improve the efficiency of the algorithm. The given method may be adopted to the description of another non-linear phenomena, accompanying the MT carrier transport, such as the carrier recombination. The results of MC calculations of thermally stimulated currents in the presence of bimolecular recombination have been yet published [10].

## 2. Formulation of the problem

### 2.1 SPD method

For the exemplary presentation of MC algorithm let us consider the isothermal SPD method. It consists in the following. The sample of investigated photoconductive solid has a form of plane plate of thickness  $L$ . The bottom surface ( $x = L$ ) is in contact with a grounded electrode. Initially, a total charge  $Q_0$  is deposited on the upper surface ( $x = 0$ ); the corresponding surface potential being equal to  $V_0$ . At a moment  $t = 0$  the upper surface is illuminated by a short light pulse and a charge  $Q_{in} = \eta Q_0$  is injected into the sample ( $\eta$  — the injection efficiency,  $0 < \eta \leq 1$ ). The motion of charge carriers in the sample towards opposite surface results in the gradual decay of an electric field  $E(x, t)$  and a surface potential  $V(t)$ , which value is monitored in the experiment (open-circuit configuration). The boundary condition for the field at injecting electrode has then the form

$$E(0+, t) = E_{in} = \eta V_0 / L. \quad (1)$$

In the MC simulation the space charge in the sample is approximated by a large number  $N$  of infinitesimally thin carrier sheets, having the charges  $q_0 = \eta Q_0 / N$ . For simplicity, in sections 3-6 these sheets will be called 'carriers'. According to Gauss theorem, the field acting on  $r$ -th carrier sheet, as counted from injecting electrode, equals to

$$E_r = E_{in} + (r - 0.5)\Delta E, \quad (2)$$

where

$$\Delta E = \frac{\eta V_0}{NL}. \tag{3}$$

The displacement  $\Delta x$  of a single carrier sheet and the resulting potential decay  $\Delta V$  are interrelated by

$$\Delta V = \frac{\eta V_0}{N} \frac{\Delta x}{L}. \tag{4}$$

### 2.2 MT carrier transport

The MT carrier transport in a solid is characterized by the following quantities: the free carrier mobility  $\mu_0$ , the mean time-of-life of a free carrier  $\tau_f = 1/C_t N_{tot}$  ( $C_t$  — carrier capture coefficient,  $N_{tot}$  — trap density per volume unit), the mean time-of-life of a trapped carrier  $\tau_r(\varepsilon) = \nu_0^{-1} \exp(\varepsilon/kT)$  ( $\varepsilon$  — trap depth,  $\nu_0$  — frequency factor,  $k$  — Boltzmann constant,  $T$  — sample temperature) and the trap density  $N_t(\varepsilon)$  per volume and energy units. As the model trap distribution, leading to dispersive transport, the exponential distribution is chosen here,

$$N_t(\varepsilon) = \frac{N_{tot}}{kT_c} \exp\left(-\frac{\varepsilon - \varepsilon_t^0}{kT_c}\right), \quad \varepsilon \geq \varepsilon_t^0 \tag{5}$$

(with  $\varepsilon_t^0$  the lower limit and  $T_c$  the characteristic temperature of trap distribution).

The MC simulation of carrier transport consists in calculating repeatedly the following random deviates: the carrier dwell-time  $\Delta t_w$  in an allowed band, the trap depth  $\varepsilon$  and the carrier dwell-time  $\Delta t_r$  in a trap. In the considered case all the deviates are distributed exponentially and their values may be obtained from the formulae (see, for example, [2]):

$$\Delta t_w = -\tau_f \ln R_1, \tag{6}$$

$$\varepsilon = \varepsilon_t^0 - kT \ln R_2, \tag{7}$$

$$\Delta t_r = -\tau_r(\varepsilon) \ln R_3. \tag{8}$$

Here,  $R_1$ ,  $R_2$  and  $R_3$  are the random deviates, distributed uniformly in the interval  $(0, 1]$ .

In the MC simulation it is assumed that all the carriers, belonging to a given sheet, have identical values of  $\Delta t_w$ ,  $\varepsilon$  and  $\Delta t_r$ . One should notice that for typical values of simulation parameters the inequality  $\Delta t_w \ll \Delta t_r$  is almost always fulfilled. This implies that the movement of more than one ‘carrier’ in the allowed band at a given moment is highly improbable and may be ignored.

In the calculations one has to choose some initial distribution of the ‘carriers’ injected into the sample. For example, one can assume the uniform ‘carrier’ distribution in a surface layer of thickness  $L_0 \ll L$ . The initial ‘carrier’ position is then given by

$$x_0 = L_0 R_0, \quad (9)$$

where  $R_0$  is the random deviate of uniform distribution in the interval  $(0,1]$ .

### 3. Basic data structures and procedures

The MT carrier transport in the presence of space charge effects has a collective character. Therefore, in the program one must store the actual positions of all carriers, as well as their release moments from the traps. If a total number  $N$  of the carriers is large, say  $N > 1000$ , attention must be paid to the proper choice of used data structures, which significantly influences the simulation efficiency.

In the presented algorithm the carriers (i. e. the carrier sheets) were enumerated by the index  $m$  ( $m = 1, 2, \dots, N$ ). The actual values of carrier coordinates and release times are stored in the arrays  $x[m]$  and  $tr[m]$ , respectively. In addition, the carrier indexes  $m$  are saved in the two binary trees, according to increasing order of  $x[m]$  or  $tr[m]$ . This means that  $x[m_{r-1}] < x[m_r] < x[m_{r+1}]$  or  $tr[m_{r-1}] < tr[m_r] < tr[m_{r+1}]$ , provided that node  $m_r$  is the 'parent' of the left node  $m_{r-1}$  and of the right node  $m_{r+1}$ . Hereafter these trees will be referred to as x-tree and t-tree, respectively. In order to speed-up the searching process, so called Adelson-Velskii and Landis (AVL) trees were utilized (see [11, 12]).

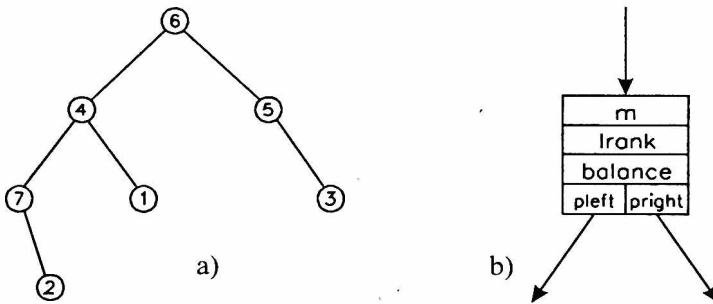


**Figure 1.** Small AVL tree (a) and structure of its single node (b). In the tree nodes only the values of 'carrier' indexes  $m$  are shown. According to (a), the sequence of indexes  $m$  corresponding to increasing order of  $x[m]$  or  $tr[m]$  is: 7, 2, 4, 1, 6, 5, 3.

The structure of the AVL tree is shown in Figure 1. It is by definition balanced, i.e. for each node the heights of its left and right subtrees may differ at the most by unity. The tree nodes are the records containing in the present case, apart from the index  $m$ , the following fields. *lrank* equals to the number of nodes in the left subtree, including the current node, whereas *balance* is the difference between the heights of the right and left subtrees. These variables are used by some procedures, operating on the tree. *pleft* and *pright* are the pointers to the corresponding nodes.

The algorithms of basic operations on the AVL trees are described in [11, 12]. In particular, the book [12] contains the procedures, written in Pascal, which may be adopted for the present purposes. The entire simulation program was also written in Pascal. The necessary operations and procedures are (for definiteness, the x-tree is considered):

- 1) insert new node, corresponding to the carrier of index  $m$ , into the tree:  
**insert**( $px, m, pxroot$ );
- 2) delete the node, corresponding to the carrier of index  $m$ , from the tree:  
**delete**( $px, m, pxroot$ );
- 3) find the index  $m$  of the carrier, which coordinate  $x[m]$  has a rank  $r$  in the increasingly ordered sequence of  $x[m_s]$ :  
**index**( $px, m, pxroot$ );
- 4) find the rank  $r$  of the carrier coordinate  $x[m]$  in the increasingly ordered sequence of  $x[m_s]$ :  
**rank**( $px, m, pxroot$ ).

Here,  $px$  and  $pxroot$  are the pointers to the array  $x[m]$  and to the x-tree root, respectively. An important feature of the AVL tree is that the time of each operation increases with a number  $N$  of nodes as  $\log N$ . If solely the array  $x[m]$ , ordered or not, was used to store the carrier coordinates, some of the operations would require the time proportional to  $N$ .

The obtained values of the function  $V(t_{i+1}) - V(t_i)$ , averaged over the time intervals  $\Delta t_i = t_i - t_{i-1}$  ( $i = 1, \dots, K$ ), are saved in the array  $DV[i]$ . Since the isothermal SPD curves are usually presented in double logarithmic scale, it is convenient to choose the width of time intervals according to

$$\Delta t_1 = (p-1)t_0, \quad (10)$$

$$\Delta t_{i+1} = p\Delta t_i, i > 0, \quad (11)$$

where  $p = (t_K/t_0)^{1/K}$  ( $t_0$  and  $t_K$  — the initial and final limits of the time scale).

## 4. Simulation of isothermal SPD

In the MC simulation one can assume that the MT carrier transport consists of the *successive* displacements of individual free carriers in the sample (cf. section 2). For this reason the simulation algorithm is rather simple. The following steps may be distinguished.

### 1. Initialization of calculations

Calculate the initial ( $t = 0$ ) positions  $x[m]$  and release times  $tr[m]$  of all the carriers ( $m = 1, \dots, N$ ), using Eq. (9) and Eqs. (7)-(8). Store the carrier indexes in the x- and t-trees. Set the elements of the array  $DV[i]$  equal to zero.

## II. Main loop of algorithm

1) Find the carrier with a minimum release time  $tr[m]$ . If there is no carriers in the sample or  $tr[m] > t_k$ , go to III).

2) Calculate the free carrier time-of-life  $\Delta t_r$  from Eq. (6) and determine the carrier displacement  $\Delta x$ . The field  $E_r$ , acting on the carrier, is given by Eqs. (2)-(3). Three cases must be distinguished.

a) If the carrier does not encounter any of the trapped carriers and does not reach the grounded sample surface then

$$\Delta x = \mu_0 E_r \Delta t_r, \quad (12)$$

where  $r$  is the rank of moving carrier.

b) If the carrier encounters some number  $s$  of the trapped carriers (with indexes  $m_{r+1}, \dots, m_{r+s}$ ) and does not reach the opposite sample surface then

$$\Delta x = x[m_{r+s}] - x[m] + \mu_0 E_{r+s} \left( \Delta t_r - \sum_{l=r+1}^{r+s} \Delta t_l \right), \quad (13)$$

where

$$\Delta t_l = (x[m_l] - x[m_{l-1}]) / \mu_0 E_{l-1}, \quad (14)$$

$r$  is the initial rank of moving carrier and  $m_r \equiv m$ .

c) If the carrier reaches the grounded sample surface then

$$\Delta x = L - x[m]. \quad (15)$$

3) Identify the time interval, in which the carrier release event took place (cf. Eqs. (10)-(11)). Increment the corresponding element of the array  $DV[i]$  by the value  $\Delta V$ , given by Eq. (4).

4) If the carrier still remains in the sample, calculate the trapped carrier time-of-life  $\Delta t_r$  from Eqs. (7)-(8) and update the carrier position  $x[m]$ , the release time  $tr[m]$  as well as the x- and t-trees. Otherwise delete the carrier index from x- and t-trees.

5) Simulate the motion of subsequent carrier, that is go to 1).

## III. Printout of results

For all the time intervals print the values of  $\log[(t_{i-1} + t_i)/2]$  and  $\log [DV[i]/\Delta t_i]$ . This yields the table (histogram) of  $\log[-dV(t)/dt]$  vs  $\log(t)$ .

The aim of the above description is to illustrate the main ideas of used MC algorithm. Therefore, some oversimplifications have been made. Among others, the MC method enables us also to obtain the spatial and energetic distributions of trapped

carriers and the spatial field distribution at given times. In the program, the dimensionless variables have been used, which reduces the number of simulation parameters.

## 5. Simulation of MT transport under another conditions

The described MC method may easily be adopted to the investigation of MT carrier transport, influenced by space charge, in another conditions. Basic modifications of the algorithm, corresponding to some experimental methods, are indicated below.

### 1) Constant-voltage configuration

The dispersive transport is most frequently studied in the constant-voltage configuration. A sample is sandwiched between two electrodes and a constant external voltage  $V_0$  is applied to the sample. The carriers are either a) generated in the sample by a short light pulse or b) continuously injected into the sample, subject to the condition  $E(0+,t) = E_{in} = 0$ . The current transients, induced in the external circuit, are respectively called a) space-charge-perturbed currents (SCPC) and b) transient space-charge-limited currents (TSCLC) [13].

In the MC simulation the continuous carrier distribution is again replaced by the set of  $N$  carrier sheets with the charges  $q_0 = \eta Q_0 / N$  ( $Q_0$  — the charge on the electrode,  $\eta = 1$  for TSCLC). The field  $E_{in}$  at the injecting electrode is determined from the condition

$$\int_0^l E(x,t) dx = V_0, \quad (16)$$

Since the electric field between separate carriers is uniform, the above integral is easy to calculate. In the case of TSCLC, the rigorous boundary condition is replaced by

$$0 \leq E_{in} < \Delta E, \quad (17)$$

where  $\Delta E$  is given by Eqn. (3). If the above inequality does not hold, new carriers are injected into the sample at  $x \approx 0$ . The current intensity  $I(t)$  in external circuit can be determined using the relationship

$$\Delta Q = \frac{\eta Q_0}{N} \frac{\Delta x}{L}, \quad (18)$$

where  $\Delta Q$  is the charge flowing in the circuit.

### 2) Non-isothermal regime

Apart from the experimental techniques considered above, the non-isothermal dispersive transport is also investigated (e.g. [14]), both in the open-circuit and constant voltage configurations. Usually the sample temperature  $T(t)$  is increased linearly with time.

The most distinguishing feature of the non-isothermal MT transport, as compared with isothermal one, is the gradual decrease of mean time-of-life of trapped carriers,  $\tau_r(\varepsilon, t) = v_0^{-1} \exp[\varepsilon/kT(t)]$ . The temperature dependencies of other transport parameters are of minor importance. The above MC algorithms may be thus adopted to the description of thermally stimulated phenomena by a suitable change of Eq. (8), which determines the carrier dwell-time  $\Delta t_r$  in a trap. In the non-isothermal case, the distribution function of  $\Delta t_r$  has the form of

$$F(\Delta t_r) = 1 - \exp \left[ - \int_{t_r}^{t_r + \Delta t_r} \frac{dt}{\tau_r(\varepsilon, t)} \right], \quad (19)$$

where  $t_r$  is the moment of carrier capture. The value of  $\Delta t_r$  can be obtained from the implicit equation  $F(\Delta t_r) = R_3$ , where  $R_3$  is the random deviate of uniform distribution in (0,1]. The method of solving numerically this equation was given in [15]. Another technique of generating the deviate  $\Delta t_r$  was described in [16].

## 6. Numerical results

The numerical results given below have preliminary character. In the Figures 2-4 the results of MC simulation are compared with those following from the approximate solutions of MT equations [3-5]. The numerical and analytical curves are denoted by points and full lines, respectively. Except for Fig. 4, the results concern three injection levels  $\eta$  of the carriers. Figures 2 and 3 show the isothermal SPDs and SCPCs, respectively. One can recognize that the space charge affects mainly the shape of the final part of SPD curve, as well as of the initial part of SCPC curve. Figure 4 presents the TSCLC and, for comparison, the SCPC corresponding to the maximum injection

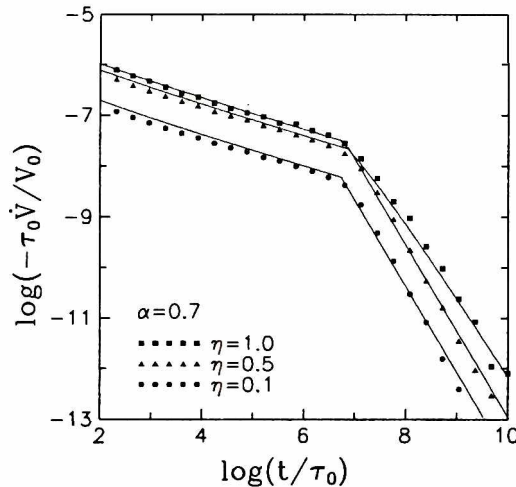


**Figure 2.** Isothermal SPD transients calculated by the MC method and computed analytically. The parameters:  $\tau_r/\tau_0 = 2 \times 10^5$ ,  $v_0\tau_0 = 1.0$ ,  $\varepsilon_0/kT = 0.0$ ,  $L_0/L = 10^4$ ,  $N = 1000$ .  $\alpha = T/T_c$ ,  $\tau_0 = L^2/\mu_0 V_0$



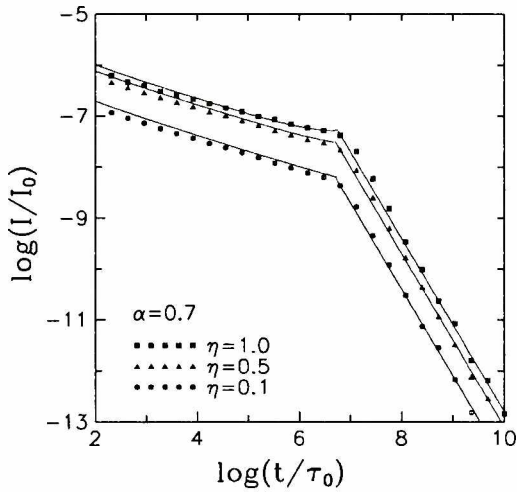


**Figure 3.** Isothermal SCPC transients calculated by the MC method and computed analytically. The values of parameters and the notations are as in Fig. 2.  $I_0 = Q_0 / \tau_0$ .

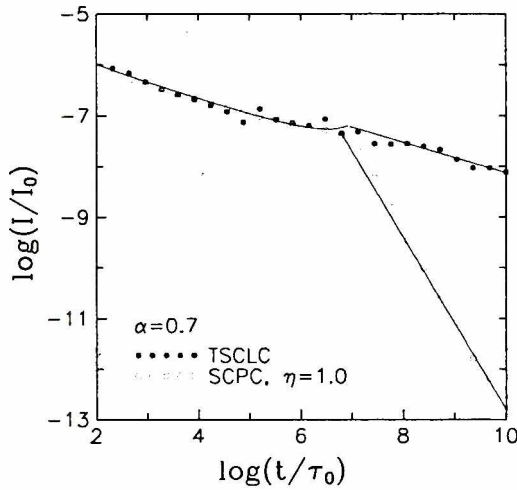


**Figure 4.** TSCLC and SCPC transients calculated by the MC method and computed analytically. For TSCLC  $N=40$ . The values of other parameters and the notations are as in Fig. 2.  $I_0 = Q_0 / \tau_0$ .

level  $\eta = 1$ . In the initial time region, both current transients are almost identical. Despite some numerical fluctuations there exists rather good agreement between all the Monte Carlo and analytical results. This proves to a certain degree the correctness of the used algorithms.

It is of some importance to test the efficiency of the described MC technique.

As follows from the remark in section 3, the execution time  $t_{exe}$  of the programs should increase with the carrier number  $N$  as  $t_{exe} \propto M \log N$ . The results of performance tests, concerning the simulation of SPD, are given in Figure 5. It is seen that the  $t_{exe}$  vs  $M \log N$

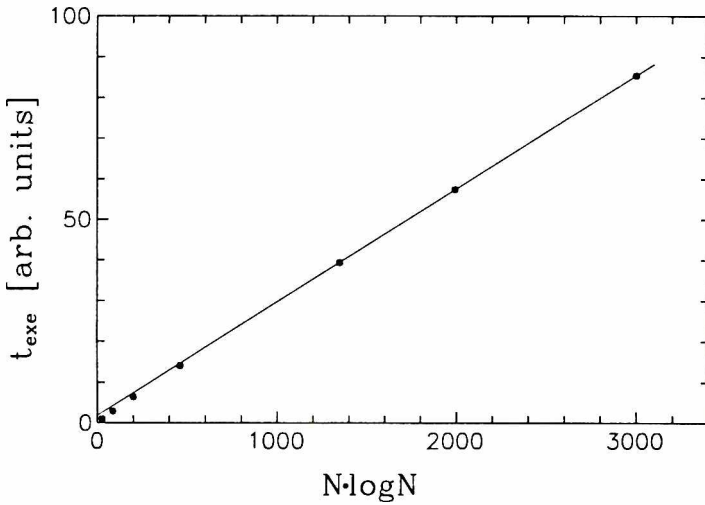


*Figure 5. Execution time of the program calculating SPDs for different number  $N$  of 'carriers'. The values of other parameters as in Fig. 2.*

plot become in fact linear for larger  $N$ . The results obtained in the case of SCPC are very similar. This indicates the satisfactory efficiency of the used algorithms. Their possible refinements may reduce only the proportionality constant between  $t_{exe}$  and  $M \log N$ .

## 7. Conclusions

In the paper the MC method of simulation of MT carrier transport, taking into account the space-charge effects, is described. The considered algorithm seems to be fully reliable, highly effective, and may be easily adopted to the study of carrier transport at various conditions. The preliminary numerical results support these statements.

### *Acknowledgement*

The author gratefully acknowledges Dr. J. Rybicki for encouragement to publish the paper in the TASK Quarterly.

### *References*

- [1] Pfister G. and Scher H. 1978 Adv. Phys. **27** 747
- [2] Marshall J. M. 1977 Phil. Mag. **36** 959
- [3] Arkhipov V. I. and Rudenko A. I. 1982 Sov. Phys.-Semicond. **16** 1153

- 
- [4] Silver M., Snow E., Wesson D., Okamoto K., Konenkamp R. and Hermann M. A. 1984 *J. Non-Cryst. Solids* **66** 237
  - [5] Tomaszewicz W. 1985 *Proc. 5th Intern. Symp. Electrets Heidelberg* 322
  - [6] Fleming R. J. 1979 *J. Appl. Phys.* **50** 8075
  - [7] Naito H., Motomura K., Okuda M., Nakau T. and Matsushita. T. 1984 *J. Appl. Phys.* **23** 296
  - [8] Tomaszewicz W. 1995 *Proc. 10th Natl. Conf. Molecular Crystals 95 Poznań P-31* (in Polish)
  - [9] van Swaaij R. A. C. M. M., Elmer S. J., Willems W. P. M., Bezemer J., Marshall J. M., Hepburn A. R. 1993 *J. Non-Cryst. Solids* **164-166** 533
  - [10] Tomaszewicz W., Rybicki J. and Grygiel P. 1997 *J. Non-Cryst. Solids* **221** 84
  - [11] Knuth D. E. 1973 *Sorting and Searching The Art of Computer Programming Addison-Wesley: Reading MA* Vol. 3
  - [12] Wirth N. 1976 *Algorithms + Data Structures = Programs* Prentice-Hall: Englewood Cliffs New Jersey
  - [13] Lampert M. A. and Mark P. *Current Injection in Solids* Academic Press: New York
  - [14] Stasiak M., Jeszka J. K., Zieliński M., Plans J. and Kryszewski M. 1980 *J. Phys. D: Appl. Phys.* **13** L221
  - [15] Tomaszewicz W. 1992 *J. Phys.: Condens. Matter* **4** 3967, 3985
  - [16] Mandowski A. and Świątek J. 1992 *Phil. Mag.* **B 65** 729